Magnetoelastic Effects in $KMnF_3$

I. Maartense and C. W. Searle
Department of Physics, University of Manitoba, Winnipeg, Canada
(Received 23 February 1972)

Measurements on $KMnF_3$ have revealed several anomalies in the magnetic susceptibility near $T_N = 87.9$ °K. When a crystal is cooled below T_N a small field-dependent susceptibility component, saturating at ~100 Oe, is seen; near $T_N - 1$ °K this component disappears; it is much weaker upon subsequent warming, but recovers when the sample is again cooled from slightly above T_N; a negative-field hysteresis and a low-frequency oscillatory behavior are also observed. Since this anomaly is much smaller in powdered samples, it is assumed to be associated with a weak moment induced by residual local stresses, caused by the crystallographic distortion at T_N. A more basic property of the bulk material, seen in all samples, is an increase of ~8% in the antiferromagnetic susceptibility below T_N; the data are inconsistent with an exchange-magnetostriction mechanism. Many of the experimental results, including those of Heeger, Beckman, and Portis can be explained in terms of a magnetoelastic coupling mechanism. When the effective elastic constant, for strains which result in magnetic canting, is very low, then a large enhancement in the transverse antiferromagnetic susceptibility is expected, and a field-induced canting transition can occur. This transition and the first-order canting transition at $T_c \approx 82$ °K will occur in the present model only if a stable crystallographic state with a spontaneous strain exists independently of magnetic interactions, at low temperatures. In samples of decreasing particle size, the width and thermal hysteresis of the canting transition increase until in particles ~25 μm and smaller, the canted state can persist up to T_N. The measured canted moment at 77 °K is 9.6 emu/mole, approximately half the low-temperature value, which suggests that the canting angle of the antiferromagnetic sublattices is practically constant below T_c. It is proposed that an observed abrupt decrease in the ultrasonic attenuation below T_c is due to magnetoelastic propagation of sound waves across the crystallographic domain walls, which above T_c cause a large amount of scattering and attenuation.

I. INTRODUCTION

The basic crystallographic[1,2] and magnetic[3,4] properties of $KMnF_3$ have been known for some time. Two structural transitions are found to occur in this perovskite-type crystal, and the transition from the high-temperature cubic phase to a tetragonal phase[5] near 184 °K has recently received much attention.[6] The second transition, near 88 °K, to orthorhombic or monoclinic symmetry[1,2] has been less extensively studied, probably because of the additional complication owing to the antiferromagnetic order[7] which sets in at this temperature. It has been assumed[3] that this is a first-order transition and is driven by exchange magnetostriction, although there is no experimental evidence in support of this assumption.

A further instability of the crystal structure is indicated by the existence of a magnetic canting transition[3] near 82 °K, which appears to be associated with a displacement of the fluorine ions but not with a change in lattice constants.[1] The distortion of the fluorine octahedra, surrounding the magnetic Mn^{2+} ions, can cause[8] effective anisotropy fields which are noncollinear at sites of opposite Mn spins; this type of single-ion anisotropy leads to a small amount of canting of the antiferromagnetic sublattices[3] below ~82 °K, resulting in a weak ferromagnetic moment. The over-all behavior of $KMnF_3$ seems to have a number of features in common with that of $RbFeF_3$. However, in the latter material, one of the lattice distortions appears to be driven by a Jahn-Teller type of instability in the Fe^{2+} ions[9]; this factor, at least, is absent in the S-state Mn^{2+} ions.

Our interest in $KMnF_3$ arose out of some anomalous results obtained by means of ac susceptibility measurements in low fields, especially a strange field-dependent behavior superposed on a field-independent step in the susceptibility just below the Néel point. Consequently, the temperature region including T_N and the canting transition has been studied in single crystals and in powders of various particle sizes. The results common to all samples below T_N have been interpreted in some detail, since they can be related to basic microscopic processes. It has been possible to explain many of the experimental results, including those of Heeger *et al.*,[3] by using a simple magnetoelastic model. An ultrasonic propagation experiment has given additional information on the canting transition in the crystal.

II. EXPERIMENT AND RESULTS

In order to eliminate sample-dependent effects in our results as much as possible, $KMnF_3$ sam-

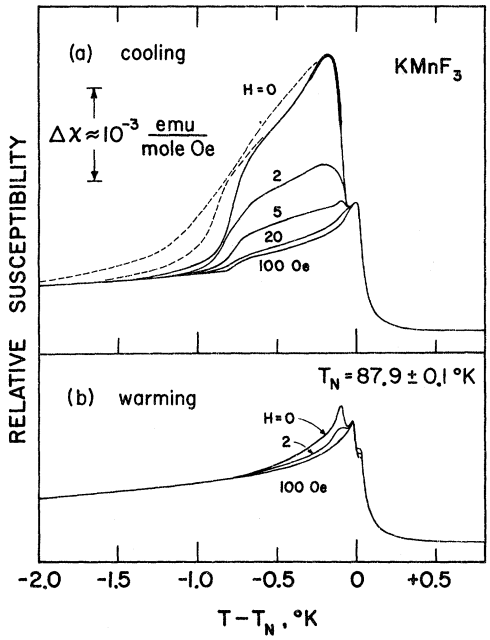

FIG. 1. Susceptibility at 10 MHz of a $KMnF_3$ crystal, with the rf field and a biasing field $\vec{H}$ applied parallel to a ⟨100⟩ direction. (a) Temperature decreasing. The broken curves show the initial susceptibility for the first two coolings in an experiment; the thickened segment of the $H=0$ curve locates the region of oscillatory behavior of the susceptibility. T_N is here defined by the field-independent maximum. (b) Temperature increasing. The minimum temperature during cycling was about 4 °K belo T_N; the small steps at T_N do not have a reproducible fiel dependence.

ples from different sources were investigated, in single crystal and powder forms. Since no differences other than those due to crystallite size were found, the behavior reported here is considered to be a property of the $KMnF_3$ structure. The single-crystal results, described below, were obtained from a sample ~1 cm^3 in size, supplied by MRC.[10] The unusual behavior near T_N was first noted in a slightly smaller crystal obtained from Semi-Elements.[11] Powdered material from the latter source was separated into fractions with different average particle sizes.

The rf susceptibility at 10 MHz was recorded, as a function of either temperature or applied field, in a manner previously described.[12] The rf field strength was ~0.1 Oe rms; biasing fields up to 100 Oe were applied parallel to the rf field direction. Data taken at 200 kHz do not show any effects which can be attributed to the 50-to-1 change in frequency. Ultrasonic measurements were made at 10 MHz using conventional pulse techniques. Longitudinal waves were generated by a quartz transducer bonded to a {100} face of the crystal by means of indium-tin solder[13]; this bond allowed temperature cycling through the crystallographic transitions of the sample without loss of acoustic contact.

The magnetic anomaly, as seen in temperature and field sweeps of the single crystal with the external field along a ⟨100⟩ direction, is shown in Figs. 1 and 2. The traces in Fig. 2 were recorded while the sample temperature decreased slowly. The large low-field susceptibility "spikes" occur only within a small temperature interval (~1 °K) and only when cooling below the Néel point, $T_N = (87.9 \pm 0.1)$ °K, here defined by the field-independent maximum in the susceptibility [Fig. 1(a)]. The spikes are much smaller ($\sim\frac{1}{10}$) in amplitude when the crystal is warmed from below $T_N - 1$ °K [Fig. 1(b)]; when the temperature drift is reversed from cooling to warming while within the "spike region" ($T_N - 0.5$ °K, say), the spike amplitude retains the minimum value achieved during cooling. No temperature hysteresis is observed above T_N; that is, the spike behavior is recovered after the crystal is warmed only slightly (≈0.5 °K) above T_N. Further warming to ~T_N + 20 °K has no measurable effect, and no additional susceptibility anomaly is found; thus there is no evidence here of the hysteresis in the crystallographic distortion reported by Beckman and Knox.[1]

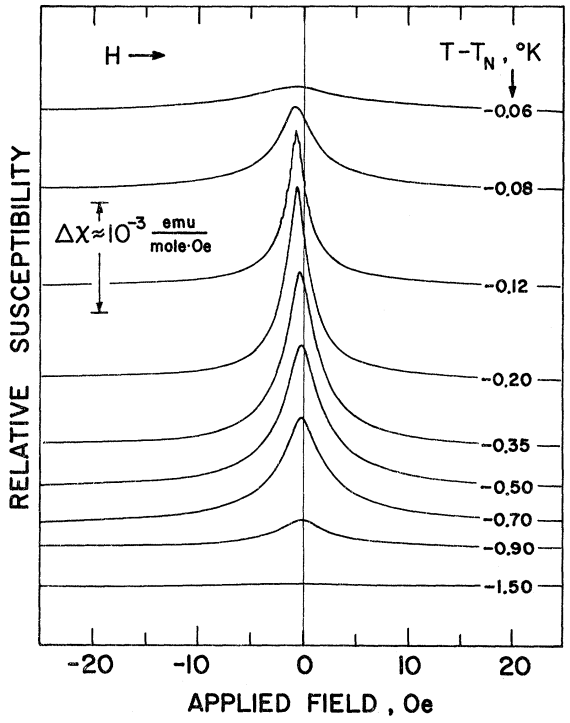

FIG. 2. Field dependence of the anomaly in Fig. 1(a); the field H is swept from left to right while the sample is cooling slowly. The recorder traces have been displaced along the vertical axis for clarity.

It should also be noted that the shape of the low-field anomaly is slightly different after thermal cycling. The broken curves in Fig. 1(a) show the zero-field behavior during the first two coolings of an experimental run; for subsequent cycles (solid curves) the changes are much smaller.

A negative hysteresis is seen in Fig. 2 for the field dependence of the spikes: The maximum susceptibility occurs before the field passes through zero. Thus, if a net magnetic moment is associated with the spikes, it changes most rapidly before the external field reverses; Fig. 3 shows H_R, taken as half the field difference between spike maxima swept in both field directions (an offset of ~0.6 Oe in the recorded data apparently results from the ambient field component parallel to h_{rf}). A rapid reduction is seen in $|H_R|$ as the temperature decreases; Fig. 3 shows a sign change in H_R near $T_N - 0.8\,^\circ$K, but this may be due to the perpendicular component of the ambient field. Where measurements with increasing temperature are possible, H_R is found to be the same during cooling and warming.

In the region of maximum $|H_R|$, just below T_N, all cooling runs show an oscillatory behavior in the spikes close to zero field. This is seen as the ripples in one of the traces of Fig. 2 and in the thickness of the zero-field trace in Fig. 1(a). The oscillations have a frequency of the order of 10 Hz and an amplitude of about 10^{-5} emu/mole Oe. It is not clear whether these oscillations are induced only by temperature or by field changes, or are a steady-state phenomenon. Experiments using precise temperature control and careful shielding of the ambient field will be necessary for further studies of this effect.

Before considering the effect of particle size on the behavior near T_N, the magnetic canting transition will be described. It is known from torque measurements[3] that a hysteresis of about 2 °K occurs between cooling and warming through this transition. This is also observed in the low-field rf susceptibility,[12] where, in addition, a dependence on thermal and magnetic cycling is noted. Furthermore, a large latent heat is associated with the transition, as shown in temperature-drift runs by the constancy of the crystal's temperature while going through the transition. No specific-heat anomaly can be seen near 88 °K with this simple method, even though a change in lattice parameters occurs there, but not at the canting transition.[1]

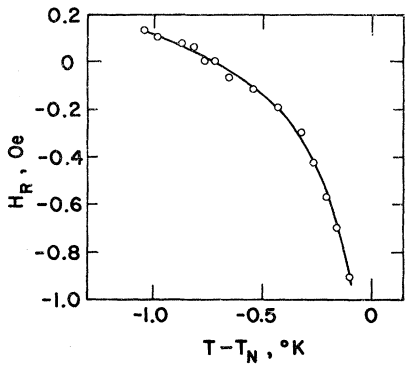

FIG. 3. Temperature dependence of the field H_R at which the susceptibility has a maximum, as in Fig. 2.

The ultrasonic propagation results show an abrupt decrease in the attenuation as the crystal cools slowly through the canting transition, while at the same time the echo pattern shifts rapidly in a random fashion, as if acoustic reflections occur from a number of moving boundaries within the sample. Below the transition the echo pattern again becomes stationary, with an attenuation about $\frac{1}{10}$ of that above the transition, that is, with a characteristic time for echo decay which is 10 times as long. Upon warming, the lossy state is rapidly reestablished; this state is seen to exist only between the canting transition and the crystallographic transition near 184 °K.

The susceptibility behavior of the powdered samples (Fig. 4) shows the following differences, relative to the single crystal. In general, all transitions are broadened in temperature, but the step at T_N is least affected; its amplitude and width change only slightly as the particle size is reduced. The temperature at this transition is constant, within experimental error. The spikes below T_N, however, are much reduced in amplitude, and persist to lower temperatures as the particles become smaller; the differences between cooling and warming are also reduced, if the samples have not been cooled to the canted state. The canting transitions broaden considerably in powdered samples. The decreased initial susceptibility in the canted region can be accounted for by the increased coercive force of the weak ferromagnetic moment, i.e., the magnetic hysteresis loops are wider in small particles. In samples of particles less than about 25 μm in size, the canted state partly remains up to the Néel point. This can be seen in Fig. 4 as the difference in height of the step at T_N between cooling and warming runs. It can also be seen that in all cases, the uncanting transition is narrower than the canting transition.

Magnetic-moment measurements made with a vibrating sample magnetometer confirm the step in the susceptibility χ at T_N. The data obtained from a 400-μm powder sample are as follows: At ~90 °K, $\chi = 1.70 \times 10^{-2}$ emu/mole Oe and at ~86 °K, $\chi = 1.84 \times 10^{-2}$ emu/mole Oe in a 1-kOe applied

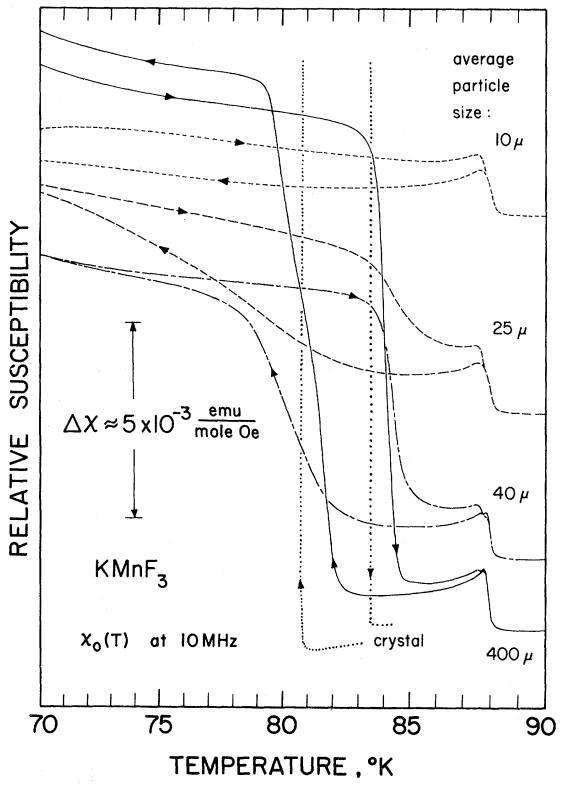

FIG. 4. Temperature dependence of the initial susceptibility of powders with various particle sizes, showing that the step at T_N is a bulk property of $KMnF_3$, whereas the canting transition is size dependent; the dotted lines locate the canting transition of a 1-cm^3 crystal. The samples were cooled to 25 °K or less. To reduce confusion, the traces have been displaced vertically.

field; the weak moment extrapolated to $T=0$, $m(0) \simeq 20$ emu/mole, and $m(77\ °K) = 9.6$ emu/mole.

III. INTERPRETATION

It will be shown that most of the complicated magnetic behavior, seen at and below T_N, can be explained in terms of a magnetoelastic coupling between an external field and a distortion of the fluorine octahedra, via the basic antiferromagnetic structure of this material. The strongest evidence for this interpretation is found in the discontinuity of the susceptibility at T_N, which is a basic property of all the samples investigated. Before considering this mechanism, we will show previous explanations to be inconsistent with experimental data obtained by different methods.

The discontinuity at T_N, which was also observed in torque measurements, was analyzed by Heeger *et al.*[3] in terms of exchange magnetostriction.[14] A strain-dependent Mn-F-Mn exchange interaction could lead to a nominally first-order magnetic transition at T_N, and a change in the crystal-lattice parameters is known to occur near there,[1,2] although there is very little change in the actual Mn-F-Mn bond angles and distances.[2] The lack of any observed temperature hysteresis at T_N could be due to the effect being very small, making the transition experimentally continuous; the latent heat at T_N could then also be small, as suggested by the present experiments. There are, however, more serious objections to the exchange-magnetostriction hypothesis for $KMnF_3$.

Firstly, the neutron-diffraction work of Cooper and Nathans[15] does not reveal an anomaly in the sublattice magnetization M which is found to follow the usual power law $M \propto (T_N - T)^{\beta}$, with $\beta \approx \frac{1}{3}$, down to at least 10 °K below T_N. A discontinuity of at least 10% should be expected at T_N.[3]

Secondly, the measured susceptibility *increases* by about 8% on cooling through T_N. In the molecular-field approximation, this would imply a *decrease* of about 12% in the exchange constant below T_N. Such a decrease is not consistent with the exchange-magnetostriction mechanism or any other known theory of magnetic ordering.

The remote possibility that the step at T_N is due to the presence of a small hard ferromagnetic component in the magnetization is ruled out by the torque data,[3] which show only a quadratic field dependence for fields below 6 kOe.

The canting transition at $T_c \approx 82$ °K is a first-order transition experimentally with a large latent heat and temperature hysteresis, and thus may appear to provide a clearer example of an exchange-driven crystal strain. But, again, no magnetic discontinuity is seen in neutron-diffraction experiments.[15]

It will be assumed, and later justified, that the anomalous magnetic behavior is the result, rather than the direct cause, of the crystallographic instabilities at T_N and T_c. In other words, distortions similar to those which are observed would occur even without the presence of magnetic ordering.

A. Simple Model

We will now describe a magnetoelastic model which can explain most of the observed magnetic phenomena, within the framework of molecular-field theory. The free energy per mole, in terms of the antiferromagnetic sublattice magnetization $M = |\vec{M}_1| = |\vec{M}_2|$, the molecular-field constant λ, anisotropy constants K_1 and K_2,[3] and an applied field $\vec{H}$, is written

$$E = \lambda \vec{M}_1 \cdot \vec{M}_2 - \frac{K_1}{2M^2}(M_{1z}^2 + M_{2z}^2) - \vec{H} \cdot (\vec{M}_1 + \vec{M}_2)$$

$$- \frac{\delta K_2}{M^2}(M_{1x}M_{1z} - M_{2x}M_{2z}) + c\delta^2 . \quad (1)$$

The fourth term represents the magnetic canting

energy owing to single-ion anisotropy, which is taken to be linearly dependent on a strain parameter δ. This parameter is normalized to the distortion coordinate ϵ of the fluorine octahedra in the spontaneously canted state, as defined by Heeger *et al.*[3] Here we consider only the magnetically induced part of the distortion of the octahedra, away from the crystallographically established equilibrium. The last term in Eq. (1) is the elastic energy associated with the induced strain; c is an appropriate elastic constant, which must be small if we are to have observable magnetoelastic effects in this model. Not included in the free energy of Eq. (1) is the temperature-dependent lattice energy $E_l(T)$, which leads to the crystal structures with $\epsilon = 0$ between T_c and T_N[3] and $\epsilon \neq 0$ (equivalent to $\delta = 1$) below T_c. It is not important, in the simple model, whether the condition that $\epsilon = 0$, in the region below T_N, reflects the static equilibrium positions of the fluorine ions, or is a spatial or dynamic average of the true distortions of the octahedra, as long as the canting term in Eq. (1) is allowed by the crystal symmetry. The assumption of a spatial variation within the magnetic unit cell giving $(\epsilon)_{av} = 0$ would imply a four-sublattice antiferromagnetic structure with hidden canting.[16]

B. Uncanted State

The equilibrium values of the sublattice canting angle α and the induced strain δ, in the case of $\epsilon = 0$, are found by minimizing Eq. (1) with respect to α and δ, taking $\alpha \ll 1$. With $\vec{H}$ applied along the x axis, i.e., perpendicular to the antiferromagnetic z axis, with $K_1 > 0$ in Eq. (1), we get

$$\alpha = \frac{M_{1x}}{M} = \frac{M_{2x}}{M} = H\left(2\lambda M + \frac{K_1}{M} - \frac{K_2^2}{M_c}\right)^{-1} = \alpha(H) \tag{2}$$

and

$$\delta = (K_2/c)\,\alpha = \delta(H)\,. \tag{3}$$

In this case, as long as the denominator in Eq. (2) is nonzero, the magnetic interactions do not cause a spontaneously induced strain (with $H = 0$) to lower the energy by canting at the expense of exchange and elastic energy, in the manner of a Jahn-Teller effect. The important result is that the transverse susceptibility is now

$$\chi_\perp' = \frac{2\alpha M}{H} = \frac{1}{\lambda}\left(1 + \frac{K_1}{2\lambda M^2} - \frac{K_2^2}{2\lambda M^2 c}\right)^{-1}. \tag{4}$$

Writing Eq. (4) in terms of the usual effective exchange, anisotropy, and canting fields, $H_E = \lambda M$, $H_A = K_1/M$, and $H_D = K_2/M$, we have, with $H_A \ll H_E$,

$$\chi_\perp' \approx \chi_\perp\left(1 - \frac{H_D^2}{2H_E H_S}\right)^{-1} \approx \chi_\perp\left(1 + \frac{H_D^2}{2H_E H_S}\right). \tag{5}$$

Here $\chi_\perp = 1/\lambda$ is the normal antiferromagnetic susceptibility, which can be obtained from measurements slightly above T_N. $H_S = c/M$ is defined as an effective strain-anisotropy field; its value can be determined from the measured enhancement $\Delta\chi_\perp = \chi_\perp' - \chi_\perp$, below T_N, since H_D can be found from the measured weak moment for $T < T_c$.

In the molecular-field theory $\chi_\perp$ is constant below T_N, and thus any temperature dependence of $\chi_\perp'$ must come from a variation in the enhancement factor of Eq. (5). The susceptibility parallel to the antiferromagnetic axis will not be changed by the magnetoelastic interaction, since $\delta(\vec{H} \parallel \vec{z}) = 0$, and it will rise from $\chi_\parallel(0) = 0$ to $\chi_\parallel(T_N) = \chi_\perp$, as usual. The idealized behavior with a temperature-independent $\chi_\perp'$ is drawn in Fig. 5. The predicted discontinuity in $\chi_\perp' - \chi_\parallel$ at T_N thus provides a ready explanation of the torque discontinuity found in $KMnF_3$ by Heeger *et al.*,[3] without invoking the exchange-magnetostriction mechanism,[14] which has been shown to be inconsistent with the available experimental data.

To estimate the value of c, the results given at the end of Sec. II may be used. These data have been obtained from a powdered sample, but their values in a single crystal will be essentially the same, because of the twinned crystal structure.[1,2] There is no conclusive information on the directions of the magnetic moment in the canted state[3,16] and on the stability of the distortion directions in the orthorhombic structure below T_N; that is, it is not known whether the orthorhombic axes can be made to assume several equivalent directions

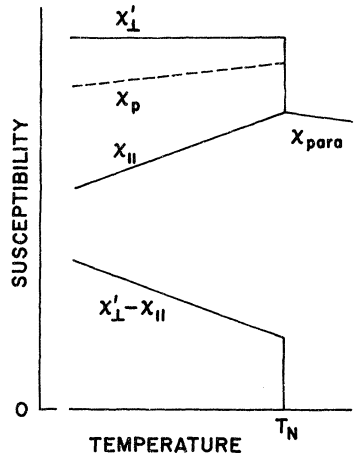

FIG. 5. Schematic description of the susceptibility behavior in the molecular-field model of a uniaxial antiferromagnet where $\chi_\perp$ is enhanced by magnetoelastic coupling; χ_P is the susceptibility of a polycrystalline sample or a heavily twinned crystal; the anisotropy $\chi_\perp' - \chi_\parallel$ will result in a torque discontinuity at T_N, as seen by Heeger *et al.* (Ref. 3).

relative to the pseudocubic axes in an applied field, as in $RbFeF_3$.[9] Thus, the measured weak moment $m(T)$ may represent ~50–100% of its true value, while $\Delta\chi_\perp \approx 1.4\times10^{-3}$ emu/mole Oe may be $\frac{1}{3}$ or $\frac{2}{3}$ of the correct value, since the antiferromagnetic axis coincides with the pseudocubic ⟨100⟩ crystal axis in the uncanted state below T_N.[3] However, these uncertainties will tend to cancel in the calculations. If we arbitrarily take $\Delta\chi_\perp(T)$ to be constant between T_N and T_c and use Eq. (5) with the appropriate values of the effective fields (see below for the calculation of H_D) then $c(T_c) \approx 3\times10^4$ erg/mole.

The field-induced canting transition, seen in torque measurements,[3] can also be treated within the present model. The magnetoelastic component of the susceptibility $\Delta\chi_\perp$ will lead to an increasing induced strain until, in a critical field H_c, $\delta=1$, which is equivalent to the spontaneous strain below T_c. E_I probably has a local minimum around $\delta=1$, above T_c, and an absolute minimum below T_c. Thus we have, using Eq. (3) with $\alpha \approx H_c/2\lambda M$, $H_c = 2H_E H_S/H_D$.

Substituting the values obtained just below T_c yields $H_c \approx 7$ kOe. The close agreement with the experimental value[3] of $H_c \approx 6.5$ kOe is probably accidental; however, the physics of the situation seems clear. The observed lack of hysteresis[3] in H_c in a real crystal will result from the clamping of the canted twins at their boundaries with the uncanted twins which have $\vec{H}$ parallel to their z axis; these boundaries will act as effective nucleation sites for the uncanted state as H is decreased.

C. Canted State

When a spontaneous strain $\epsilon \neq 0$ exists, the anisotropy term δK_2 in the canting energy of Eq. (1) is replaced by $(1+\delta)K_2$. With $\vec{H}$ along the x axis, the equilibrium canting angle is $\alpha = \alpha_0 + \alpha(H)$, where $\alpha(H)$ is given by Eq. (2) and

$$\alpha_0 = \frac{H_D}{2H_E}\frac{\chi_\perp'}{\chi_\perp} = \frac{m(T)}{2M(T)}\ ; \qquad (6)$$

here $\chi_\perp'$ is the same as in the uncanted state [Eqs. (4) and (5)] while $m(T)$ is the value of the weak moment at temperature T. Thus the effective canting field is $H_D = m(T)/\chi_\perp'$, rather than the usual value $H_D' = m(T)/\chi_\perp$; this difference is caused by the magnetically induced increase of the spontaneous strain of the octahedra as the structural distortion takes place. The equilibrium value of the induced strain is

$$\delta = \frac{K_2}{c}\alpha = \frac{H_D}{H_S}\alpha = \delta_0 + \delta(H)\,, \qquad (7)$$

with $\delta(H)$ as in Eq. (3) and

$$\delta_0 = \frac{H_D}{H_S}\alpha_0 = \frac{m^2}{2c\chi_\perp'} = \frac{\chi_\perp'}{\chi_\perp}\left(\frac{\chi_\perp'}{\chi_\perp} - 1\right)\ . \qquad (8)$$

If we take $\chi_\perp'/\chi_\perp = 1.08$, as measured at T_N, then $\delta_0 \approx 0.1$; in other words, without an applied field, the magnetoelastic interaction will drive the strain ~10% beyond the amount required for crystallographic equilibrium alone, if $\Delta\chi_\perp$ has the same value above and below T_c.

This magnetoelastic amplification in the model can be used to interpret the behavior at the canting transition. As long as the structure above T_c, with $\epsilon = 0$, is crystallographically stable, there is no self-induced strain, as pointed out earlier. However, near the temperature of structural instability nucleation of the low-temperature phase with $\epsilon \neq 0$ will bring the magnetoelastic interaction into play which, together with E_I, will encourage an increase in the strain and its propagation away from the nucleation site until the whole crystal is in the canted state. A broadening of the transition region in powdered samples will result from the spread of critical temperatures among individual particles, due to a decrease in the number of nucleation sites (such as strained regions near twin boundaries) as the particles become smaller. These arguments can also be applied to the uncanting transition at the upper critical temperature, where the canted state will collapse around sites with $\epsilon = 0$. Upon warming, lack of suitable nucleation sites will allow the canted state to persist up to T_N, as is observed in the present experiment (Fig. 4) and in that of Hirakawa *et al.*[4]

The fact that a $KMnF_3$ crystal is acoustically very lossy between T_c and 184 °K is presumably the result of scattering of the elastic waves by the large number of twin boundaries present below 184 °K. There is no reason to believe that these boundaries physically disappear below T_c. A reasonable explanation for the observed decrease in the acoustic attenuation below T_c is that the magnetoelastic coupling allows an elastic wave to be propagated across twin boundaries, through modulation of the strain parameter ϵ. The shifting echo pattern seen at T_c is consistent with a process of nucleation and growth of the canted phase at T_c.

The broadening of the transition in powdered samples is the reason that the latent heat anomaly at T_c is not resolved in the measurements by Deenadas *et al.*[17] The latent heat L can be only crudely estimated in the present experiment, from the known specific heat[17] near T_c, the change in cooling or warming rate, and the width of the transition (~0.1 °K) in the single crystal. Thus we can say that $L(T_c) \gtrsim 10^7$ erg/mole. This relatively large latent heat is consistent with our assumption that the canting transition is enabled by a crystallographic instability [which allowed the use of slightly different forms of the canting term in Eq. (1) for the canted and uncanted states]. In contrast, the change in magnetic energy upon canting is only

$-\frac{1}{2}\lambda[m(T_c)]^2 \approx -3\times10^4$ erg/mole (not -60 erg/mole, as estimated in Ref. 3). Such a small energy by itself is insufficient to stabilize the canted state in the presence of thermal energies of the order of kT_c.

The present measure of $m(0)$ agrees with that derived from torque data,[3] while $m(77\ ^\circ\mathrm{K})$ is a factor of ~12 larger than the previous value.[3] The ratio $m(77\ ^\circ\mathrm{K})/m(0) \approx 0.5$ has the value expected on the basis of a normal temperature variation of the sublattice magnetization $M(T)$ and a constant canting angle α_0; this suggests that the strain ϵ is constant below T_c.

Little can be said about the temperature dependence of the elastic constant c. An abrupt change in c at the canting transition will show itself as a discontinuity in $\Delta\chi_\perp$ at T_c. It may also be noted that, for the parallel susceptibility in the canted state, the model predicts that, at $T=0$,

$$\chi_\parallel' = \frac{H_D^2}{2H_E H_A}\,\chi_\perp\left(\frac{\chi_\perp'}{\chi_\perp}\right)^2 = \left(\frac{H_D'^2}{2H_E H_A}\right)\chi_\perp \ . \qquad (9)$$

Thus $\chi_\parallel'$ is increased, due only to canting, as expected,[18] and a discontinuity, $\Delta\chi_\parallel = \chi_\parallel'(T_c) - \chi_\parallel(T_c)$, will occur at T_c. It will be possible to observe these changes only in fields high enough to saturate the weak moment below T_c. In powdered samples the discontinuities will be smeared out, as discussed above, but in small particles which remain canted when warmed to T_N, a difference between cooling and warming behavior should be seen near T_N. Such a difference is indeed observed (Fig. 4) for fine powders, and this enchancement can then be ascribed to the sum of $\Delta\chi_\parallel$ and any change in $\Delta\chi_\perp$, and the initial susceptibility of the weak moment remaining near T_N. The latter component decreases as the particles are made smaller.

Returning now to the anomalous behavior of the $KMnF_3$ crystals near T_N, the spikes seen during cooling (Figs. 1 and 2) can be explained as the field-dependent susceptibility of a net moment induced by local residual stresses (essentially a piezomagnetic moment[19]). The large change in the lattice parameters incurred in the crystallographic distortion at T_N[1,2] will result in strained regions near tetragonal twin boundaries, with $\epsilon \neq 0$, so that a spontaneous weak moment proportional to $\epsilon(T)M(T)$ can occur. The assumption that $\epsilon(T)$ can locally be nonzero over a range of temperatures below T_N is supported by Cooper and Nathans's[15] observation that the distortion takes place over an extended range, as well as the lack of exact reproducibility upon cycling through T_N.[15] The latter effect is also seen in Fig. 1(a), where the sample has acquired a history after two cyclings. A slight redistribution of the tetragonal twinning structure is probably involved here; the reproducibility of the behavior at T_c for different samples, as well as for a given sample after cycling,[12] would be similarly affected.

The decreased amplitude of the spikes, seen when the crystal is warmed [Fig. 1(b)], is expected from the reduction in the size and number of strained regions below T_N, which took place during cooling. Similar regions of local strain probably exist above T_N, upon warming, where they are not observed because there is no long-range magnetic order. The fact that the crystal needs to be warmed only slightly above T_N(~0.5 °K) to recover its normal behavior on cooling implies that the crystallographic transition, in the bulk of the material, occurs over only a narrow temperature range with little, if any, hysteresis; this contradicts the observation of Beckman and Knox,[1] but agrees with other work.[2,15]

The smallness of the spikes observed in powdered samples and their continued presence at temperatures lower than in the crystal suggest that the strained regions in small particles are fewer in number, but remain over a larger temperature interval. Since these regions should be effective nucleation sites of the canted state, the canting transition in some particles will occur at temperatures higher than T_c of a good unstressed crystal; the uncanting transition will not be nucleated at strain sites and therefore will not occur below the transition temperature of the crystal. These suggestions are consistent with the data in Fig. 4.

The details of the crystal's behavior near T_N, seen in Figs. 1 and 2, are difficult to explain. The small field-dependent peak, seen on the low-temperature side of T_N in Fig. 1(b), may represent the critical behavior[20] of the weak moment in the small number of strained regions remaining after cooling. If this is true, then either our definition of T_N is incorrect, or the local stresses cause a slight lowering of T_N. The kinks at T_N in Fig. 1(b) probably mark the location of the crystallographic transition in the bulk of the sample. The reasons for the negative H_R of the spikes (Fig. 3) and the susceptibility oscillations close to T_N are not clear, although the magnetoelastic interactions, which apparently lead to practically all other anomalous effects in $KMnF_3$, probably are also responsible for these unusual phenomena. Lastly, in comparing the actual behavior of the bulk susceptibility underlying the low-field spikes in Fig. 1 with the idealized behavior in our simple model (broked line in Fig. 5) is should be realized that the antiferromagnetic susceptibility in real materials decreases slightly at T_N and has an inflection point.[21] Thus the curvature of χ in Fig. 1 below T_N does not invalidate our assumption that $\Delta\chi_\perp$ is relatively temperature independent between T_c

and T_N.

IV. CONCLUSIONS

We have shown how a simple magnetoelastic coupling mechanism can account for most of our experimental data, as well as the torque data of Heeger *et al.*,[3] for $KMnF_3$ in the antiferromagnetic region. Whenever the crystal symmetry is such that it allows this mechanism to operate, the magnetoelastic interaction will cause an enhancement of the transverse antiferromagnetic susceptibility. The effect is easily observed in $KMnF_3$ because of the existence of a crystallographic state, below T_N, with an extremely small effective elastic constant for the shear strain which leads to magnetic canting.

In considering the transition at T_c, where spontaneous strain and canting set in, several objections must be raised against the simple assumption[3] that canting begins when the magnetic energy is large enough to equal the elastic energy of the associated distortion of the fluorine octahedra. Without additional interactions, the energy difference between canted and uncanted states is many orders of magnitude less than kT, and a static distortion would not be stable. A simple crossing of the energies of the two states would not lead to the observed first-order behavior. On either side of the crossover temperature the antiferromagnetic susceptibility would rise to a maximum at T_c; the same would be expected for the ultrasonic attenuation. Therefore, we have had to assume that the spontaneous strain which exists below ~82 °K arises from an inherent instability of the $KMnF_3$ crystal structure, while the magnetoelastic interaction acts as a perturbation.

The inclusion of higher-order terms in the free-energy expression, including the lattice energy, with an explicit temperature dependence in the constants should result in a better description of the first-order transitions; however, the present simple model is adequate for a basic description of the experimentally observed effects. Further experiments should include accurate specific-heat measurements, as well as a determination of the field and pressure dependence of T_c and the frequency dependence of the magnetoelastic component of the susceptibility caused by relaxation effects on the strain amplitude.

---

[1]O. Beckman and K. Knox, Phys. Rev. 121, 376 (1961).

[2]A. Okazaki and Y. Suemune, J. Phys. Soc. Japan 16, 671 (1961).

[3]A. J. Heeger, O. Beckman, and A. M. Portis, Phys. Rev. 123, 1652 (1961).

[4]K. Hirakawa, K. Hirakawa, and T. Hashimoto, J. Phys. Soc. Japan 15, 2063 (1960).

[5]V. J. Minkiewicz, Y. Fujii, and Y. Yamada, J. Phys. Soc. Japan 28, 443 (1970).

[6]See, for example, M. Furukawa, Y. Fujimori, and K. Hirakawa, J. Phys. Soc. Japan 29, 1528 (1970); J. M. Courdille and J. Dumas, Solid State Commun. 9, 609 (1971), and references therein.

[7]V. Scatturin, L. Corliss, N. Elliott, and J. Hastings, Acta. Cryst. 14, 19 (1961).

[8]J. J. Pearson, Phys. Rev. 121, 695 (1961).

[9]J. B. Goodenough, N. Menyuk, K. Dwight, and J. A. Kafalas, Phys. Rev. B 2, 4640 (1970), and references therein.

[10]Materials Research Corp., Orangeburg, N. Y.

[11]Semi-Elements, Inc., Saxonburg, Pa.

[12]I. Maartense, Rev. Sci. Instr. 41, 657 (1970).

[13]Cerroseal-35, Cerro Copper and Brass Co., Bellefonte, Pa.

[14]C. P. Bean and D. S. Rodbell, Phys. Rev. 126, 104 (1962).

[15]M. J. Cooper and R. Nathans, J. Appl. Phys. 37, 1041 (1966).

[16]V. Minkiewicz and A. Nakamura, Phys. Rev. 143, 356 (1966).

[17]C. Deenadas, H. V. Keer, R. V. G. Rao, and A. B. Biswas, Brit. J. Appl. Phys. 17, 1401 (1966).

[18]R. Orbach, Phys. Rev. 115, 1189 (1959).

[19]A. S. Borovik-Romanov, Zh. Eksperim. i Teor. Fiz. 38, 1088 (1960) [Sov. Phys. JETP 11, 786 (1960)].

[20]I. Maartense, Intern. J. Magnetism 3 (to be published).

[21]M. E. Fisher, Phil. Mag. 7, 1731 (1962).